SIMULATION OF PARTICLE COAGULATION IN TEMPORALLY DEVELOPING MIXING LAYERS

S.C. GARRICK, S. MODEM AND M.R. ZACHARIAH
Department of Mechanical Engineering
University of Minnesota
Minneapolis, MN 55455-0111

AND

K.E.J. LEHTINEN
Department of Physics
Helsinki University
Helsinki, 00014 Finland

Abstract. Direct numerical simulation of coagulating aerosols in two-dimensional, mixing layers are performed. The evolution of the particle field is obtained by utilizing a sectional model to approximate the aerosol general dynamic equation. The sectional model is advantageous in that there are no *a priori* assumptions regarding the particle size distribution. This representation facilitates the capture of the underlying physics in an accurate manner.

1. Introduction

Ultrafine particles play a very important role in a wide variety of physical/chemical phenomena and processes. An important application is the synthesis of nanostructured materials. There are several technologies which can be employed in the manufacture of nanoscale materials (films, particles, *etc.*) Vapor-phase methodologies are by far the most favored because of chemical purity and cost considerations. A key issue in the formation of nanoscale particles is the prevention of hard agglomerates and chemical control. A number of strategies have been attempted to minimize agglomeration(Matsoukas and Friedlander, 1991).

The dynamics of particles in turbulent flows have received some attention. The earlier works were focused on understanding the phenomenon of particle dispersion by turbulence(Riley and Patterson, 1974; Elghobashi, 1991). The influence of particle parameters on collision frequencies in a turbulent particle laden suspension leading to coagulation was considered by Sundaram and Collins (1996), who showed that the magnitude of the minimum particle collision frequency was strongly correlated with the turbulent motions at the integral scale. Reade and Collins (2000) simulated the coagulation and growth of an initially mono-disperse aerosol subject to isotropic turbulence. This work resulted in an improved understanding of the trends in the relative width of the particle size distribution and its dependence on the Stokes number and radial distribution function. However, much of the work performed thus far consider large, micron-scale particles in a Lagrangian manner which use primarily particle tracking methods. The large number of particles needed to represent the underlying physics of particle growth using Lagrangian methods render the computations infeasible for all but inhomogeneous systems.

In this work we consider the growth of nanoscale particles in a compressible, temporally developing mixing layer. The particulate phase will be accounted for using a sectional method which treats the particles in an Eulerian manner(Pyykonen and Jokiniemi, 1999; Garrick *et al.*, 2001). This approach is advantageous in that there are no *a priori* assumptions regarding the nature of the particle size distribution. We intend to use direct numerical simulations to capture the underlying physics of particle growth in a model-free manner(Givi, 1989).

2. Formulation

The flows under consideration are two-dimensional mixing layers and are governed by the compressible Navier-Stokes equations. The transport of the nanoscale particles dispersed is governed by the aerosol general dynamic equation (GDE). The equation is expressed in a discrete form as a population balance on each cluster or particle size. From a practical standpoint however such systems of equations cannot be solved explicitly except for very small particle sizes. Therefore a sectional method is used to represent the particle field as a function of space and time.

This approach effectively divides the particle size distribution into "bins," as illustrated in Fig. 1. The discrete part of the representation models nucleation and molecule-molecule interactions which lead to particle formation. A molecular cluster q_i is comprised of i molecules. Typically molecular clusters grow by the addition of one molecular unit at a time. As particles become larger they are transitioned to the sectional representation,

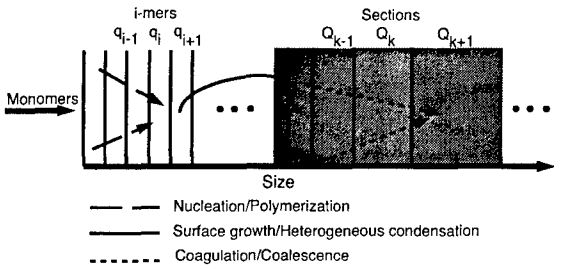

Figure 1. Discrete - sectional representation of particle field.

Q_k, after reaching a cut-off size consisting of M clusters. We consider only large clusters, and particles which typically contain tens of thousands of molecules for which a discrete representation is unnecessary. The GDE is therefore solved as a set of N_s transport equations, one for each section Q_k, $k = 1, 2, \ldots, N_s$(Xiong and Pratsinis, 1993). In adopting this framework we can write the general transport equation for the concentration of particles in the kth section, Q_k:

$$\frac{\partial \rho Q_k}{\partial t} + \frac{\partial \rho Q_k u_j}{\partial x_j} = \frac{\partial}{\partial x_j}\left(\mathcal{D}_Q \frac{\partial Q_k}{\partial x_j}\right) + \omega_k^Q, \tag{1}$$

where $\mathcal{D}_Q$ is the diffusivity

$$\mathcal{D}_Q = k_b T \frac{C_c}{3\pi\mu d_p}, \tag{2}$$

where k_b is the Boltzmann constant, C_c is the Cunningham correction factor, d_p is the particle diameter, and T and μ are the fluid temperature and viscosity, respectively. The source term, ω_k^Q, is given by

$$\omega_k^Q = \frac{1}{2}\sum_{i=1}^{N_s}\sum_{j=1}^{N_s}\beta_{i,j}\chi_{ijk}Q_iQ_j - \sum_{i=1}^{N_s}\beta_{ik}Q_iQ_k. \tag{3}$$

The source term, ω_k^Q, represents the effects of particle-particle interactions: production of Q_k due to collisions of smaller particles; the loss or gain of Q_k by collision with a smaller particle which either moves the resulting particle out of or into section k; the loss of particles in section k as they collide with each other and form larger particles; and the loss of particles in section k due to collisions with larger particles. It should be noted that repeated indices in Eq. 3 do not imply summation but instead infer interactions between

particles in section i and particles in section j. The collision frequency function β_{ij} is given by

$$\beta_{ij} = \left(\frac{3}{4\pi}\right)^{\frac{1}{6}} \left(\frac{6k_bT}{\rho_p}\right)^{\frac{1}{2}} \left(\frac{1}{v_i} + \frac{1}{v_j}\right)^{\frac{1}{2}} \left(v_i^{\frac{1}{3}} + v_j^{\frac{1}{3}}\right)^2, \tag{4}$$

where v_i is the volume of the ith particle, ρ_p is the particle density and χ_{ijk} is given by

$$\chi_{ijk} = \begin{cases} \frac{v_{k+1}-(v_i+v_j)}{v_{k+1}-v_k} & \text{if } v_k \leq v_i + v_j < v_{k+1} \\ \frac{(v_i+v_j)-v_{k-1}}{v_k-v_{k-1}} & \text{if } v_{k-1} \leq v_i + v_j < v_k \\ 0 & \text{otherwise.} \end{cases} \tag{5}$$

The sectional method is discretized in size space such that the volume of particles in two successive sections is doubled, *i.e.* $v_k = 2 \times v_{k-1}$. This scheme allows us to span a volume range of $V = v_1$ to $V = 2^{N_s-1} \times v_1$.

3. Numerical Procedure

The governing transport equations are solved using a hybrid MacCormack based compact difference scheme(Carpenter, 1990; Kennedy and Carpenter, 1994). The numerical scheme used is based on the one-parameter family of dissipative two-four schemes (DCPS)(Carpenter, 1990). The accuracy of the scheme is second order in time, and fourth order in space. All calculations are performed on a rectangular uniformly spaced grid. The computational algorithm uses the message passing interface to execute on parallel computing platforms. The treatment of the particulate phase in a Eulerian manner, as opposed to a Lagrangian one, helps to keep processor-processor communication to a minimum.

4. Results

The flows under consideration are two-dimensional, compressible, shear layers. A schematic is shown in Fig. 2. Periodic boundary conditions are used in the streamwise direction, while the free shear condition is imposed in the cross-stream direction. The gas is air, and the velocity is initialized with a hyperbolic tangent in the cross-stream direction. The Reynolds number is based on the vorticity thickness, δ_ω, and the velocity difference, $\Delta U = U_1 - U_2$, $Re_{\delta_\omega} = \frac{\Delta U \delta_\omega}{\nu}$. Two cases are considered. Case (I), considers particle coagulation in a uniform temperature flow at $T_1 = T_2 = 300K$. Case (II), considers the flow where the temperature of the particle-free stream is $T_1 = 300K$, and the temperature of the

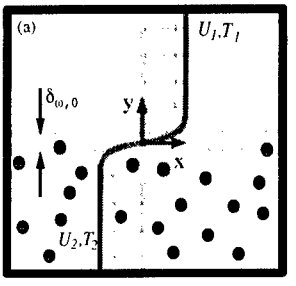

Figure 2. Flow configuration

particle-laden stream is $T_2 = 900K$. Thermophoresis effects are not included in these calculations, but inclusion of such effects pose no additional mathematical or computational difficulties(Pratsinis and Kim, 1989; Pyykonen and Jokiniemi, 1999). Both cases consider an initial volume fraction of $\mathcal{V}_f = 9.4 \times 10^{-8}$. The volume fraction is defined as the ratio of the volume occupied by the particulate phase to that occupied by the fluid. A total of ten sections are solved, *i.e.* $N_s = 10$. This allows for the solution of particles covering a range of 3 orders of magnitude in volume.

Computations are performed on a domain of $2\pi \times 2\pi$ in the streamwise, x, and cross-stream, y, directions on 1500^2 grid points. With this resolution, flows with a Reynolds number of $Re_{\delta_\omega} = 200$ are well resolved. All calculations were performed on a SGI-Origin3800 supercomputer, and each calculation simulated up to a nondimensional time of $t^\star = 14.25$.

Particle concentration profiles obtained from Case (I) are shown in Fig. 3. Cross-stream profiles of Q_1, Q_2, Q_7, and Q_{10}, are obtained by averaging in the streamwise x-direction, at four times. All values of Q are normalized by the initial number of particles in the particle-laden stream, Q_{1_o}. At time $t^\star = 0$, $Q_1/Q_{1_o} = 1$ in the particle-laden stream, and $Q_1/Q_{1_o} = 0$ in the particle free stream. Figure 3a indicates the decrease from the initial Q_1 concentration in the particle-laden stream, and increase in concentration in the initially particle-free stream. As the particles collide, they coagulate to form larger particles, thereby moving out of section 1. The increase in particles in the $y > 0$ region is due to dispersion. As the mixing layer evolves the particle-laden stream is mixed, via convection, with the particle-free fluid. The figure also reveals a peak in Q_1 near the interface of the two streams, the magnitude of which decreases with time. The peak is due to the gradient in Q_1 in the shear region which results in a lower growth rate, in comparison to that observed in the freestream of the initially particle-laden stream. A similar trend is observed in section 2, shown in Fig. 3b. Particles collide and coagulate to form larger particles which can no longer be accommodated in Q_2. The decrease of Q_2 in time is accompanied by

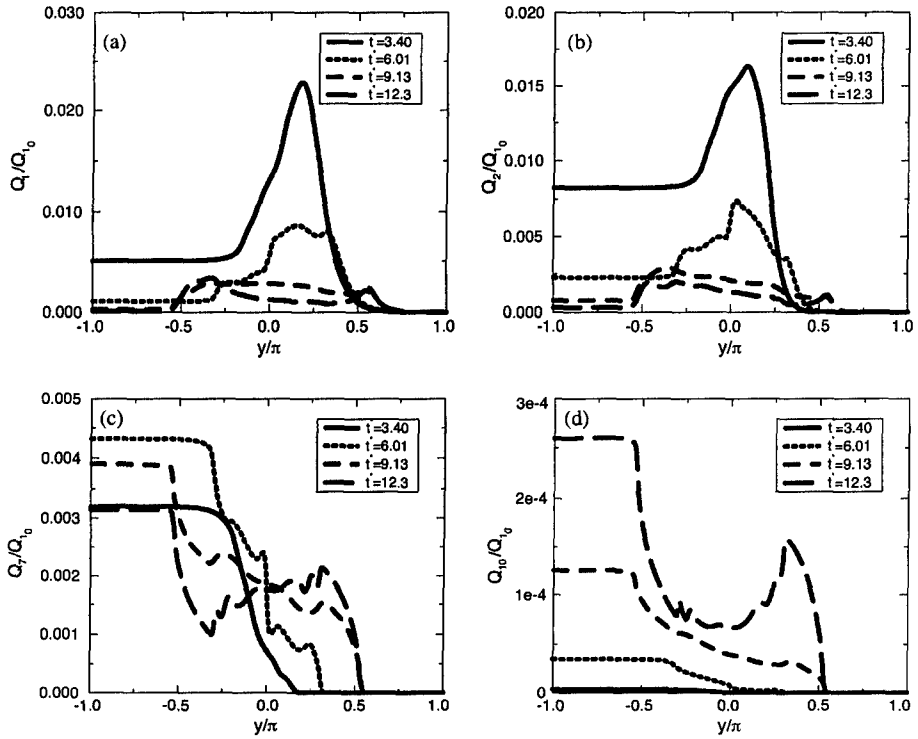

Figure 3. Cross stream variation of particle concentrations, Case (I): (a) Q_1; (b) Q_2; (c) Q_7; (d) Q_{10}.

increases in the higher numbered sections, $Q_k, k = 3, 4, \ldots, 10$. The concentration of particles in section 7 is shown in Fig. 3c. The trend is different from that observed in the first two sections in that the maximum concentration is observed in the initially particle-laden stream. The concentration increases to $Q_7/Q_{1_o} = 0.0044$, at time $t^\star = 6.01$, then begins to decrease. However, the concentration in the initally particle-free stream increases over the same period of time. Near the interface of the two streams there is some overlap of the profiles at later times, $t^\star = 6.01, 9.13$, and 12.3. This "equilibrium" may be attributed to the mixing of the particle-free stream with the particle-laden stream as the vortex develops. The concentration of particles in section 10 is shown in Fig. 3d. The figure reveals that the concentration Q_{10} increases at each y location across the mixing layer. There are fewer Q_{10} particles in the core of the vortex in comparison to the initially particle-laden stream. This further reflects the reduced growth rate observed in the first two sections. Additionally, the concentrations of all sections are seen to spread out into the particle-free stream with time as the flow develops. A qualititative view of the particle field for the isothermal flow, Case (I),

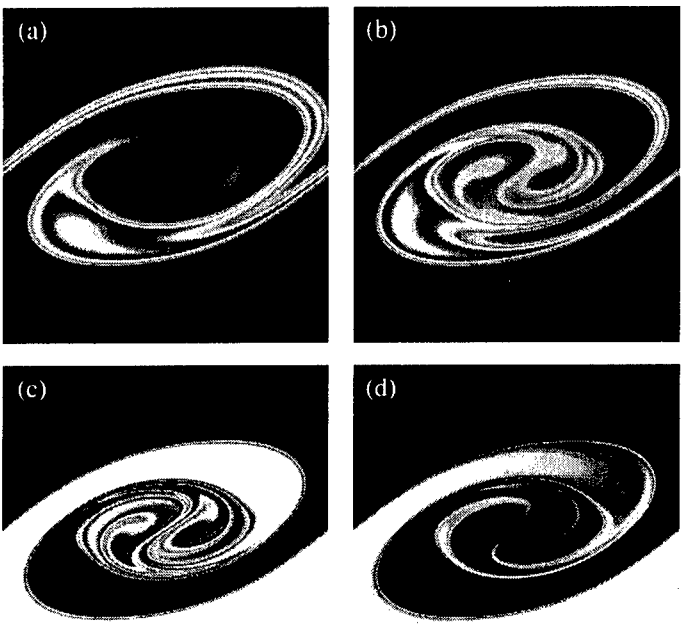

Figure 4. Instantaneous particle concentrations contours, Case (I): (a) Q_1;(b) Q_2; (b) Q_7; (b) Q_{10}.

is presented in Fig. 4. This figure shows instantaneous contours of the concentrations in sections 1, 2, 7, and 10, taken at time $t^* = 12.3$. In addition to spatial concentration variation, the diffusion effects are also evident. The striation thickness decreases as the particle size increases. This is because larger particles have smaller coefficients of diffusion.

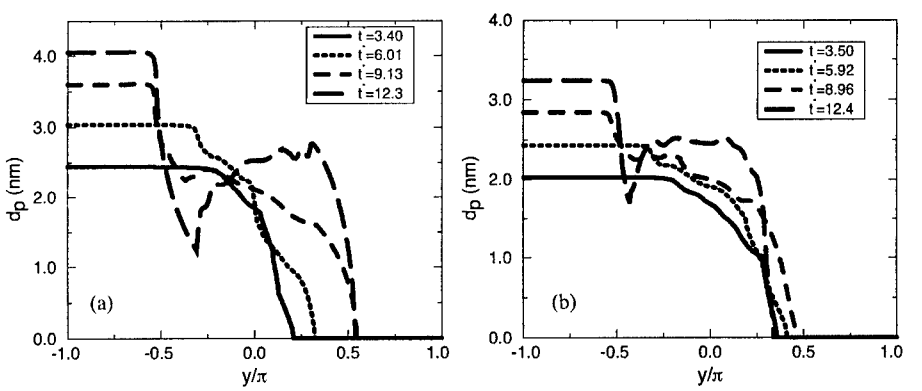

Figure 5. Cross stream variation of mean particle diameter: (a) Case (I); (b) Case (II).

Temperature effects may be observed by considering the average particle size. The average diameter is given by $d_p = (6/\pi\overline{v})^{1/3}$, where the mean volume is given by $\overline{v} = \sum_{i=1}^{N_s} Q_i v_i / \sum_{i=1}^{N_s} Q_i$. The temporal evolution of the mean diameter for Case (I), and Case (II) is shown in Fig. 5. Though the profiles show an overall increase with time, the particle growth rate in Case (II) is less than that in Case (I). Though the temperature of the particle-laden stream is greater, which also means that the rate of collisions is greater, the particles effectively grow at a slower rate. The spread of the profiles indicates mixing of the two streams as the vortices develop.

5. Acknowledgement

The first two authors acknowledge the support of the National Science Foundation under Grant ACI-9982274. Computational resources are provided by the Minnesota Supercomputing Institute.

References

Carpenter, M. H. (1990). A high-order compact numerical algorithm for supersonic flows. In Morton, K. W., editor, *Twelfth International Conference on Numerical Methods in Fluid Dynamics*, volume 371 of *Lecture Notes in Physics*, pages 254–258. Springer-Verlag, New York, NY.

Elghobashi, S. (1991). Particle-laden turbulent flows: Direct simulation and closure models. *Appl.Sci.Res.* **48**, 301–314.

Garrick, S. C., Lehtinen, K. E. J., and Zachariah, M. R. (2001). Modeling and simulation of nanoparticle coagulation in high reynolds number incompressible flows. In *Proc. Joint US Sections Meeting of the Combustion Institute*, Oakland, CA.

Givi, P. (1989). Model free simulations of turbulent reactive flows. *Prog. Energy Combust. Sci.* **15**, 1–107.

Kennedy, C. A. and Carpenter, M. H. (1994). Several new numerical methods for compressible shear-layer simulations. *Appl. Num. Math.* **14**, 397–433.

Matsoukas, T. and Friedlander, S. K. (1991). Dynamics of aerosol agglomerate formation. *Coll. Int. Sci.* .

Pratsinis, S. E. and Kim, K.S. (1989). Particle coagulation, diffusion, and thermophoresis in laminar flows. *J. Aerosol Sci.* **20**, 101.

Pyykonen, J. and Jokiniemi, J. (1999). Compuatational fluid dynamics based sectional aerosol modelling schemes. *J. Aerosol Sci.* **31**, 531–550.

Reade, W. C. and Collins, L. R. (2000). A numerical study of the particle size distribution of an aerosol undergoing turbulent coagulation. *J. Fluid Mech.* **415**, 45–64.

Riley, J. J. and Patterson, G. S. (1974). Diffusion experiments with numerically integrated isotropic turbulence. *Phys. Fluids* **17**, 292–297.

Sundaram, S. and Collins, L. R. (1996). Collision statistics in an isotropic particle-laden turbulent suspension.part 1. direct numerical simulations. *J. Fluid Mech.* **335**, 75–109.

Xiong, Y. and Pratsinis, E. S. (1993). Formation of agglomerate particles by coagulation and sintering part-i. a 2-d solution of the population balance equation. *J. Aerosol Sci.* **24**, 283–300.